Application Report
SNAA301A–January 2017–Revised May 2017

Design of Ultra-Low Power Discrete Signal Conditioning Circuit for Battery-Powered Wireless PIR Motion Detectors

Bahram Mirshab

ABSTRACT

In this document, a cost-optimized, ultra-low power op amp interface for wireless battery operated PIR (Passive Infrared) motion detectors is described. A single new 4-channel nanopower operational amplifier, TLV8544, implements the analog signal path, including two gain stages, two bandpass filters, and a window comparator.

Contents

1 Introduction 2
2 Passive Infrared (PIR) Motion Detector Sensor 2
3 Biasing PIR Sensor for Low Power Operation 4
4 Gain Stages and Band Pass Filtering 4
5 Calculation Of The Total Gain Of Stages “A” AND “B” 7
6 Window Comparator Stage 7
7 Current Consumption 11
8 Conclusion 11
9 Device Family 12
10 References 12

List of Figures

1 Block Diagram of a Wireless Battery Operated PIR Motion Detector System 2
2 (a) PIR Senor, (b) PIR Transducer, (c) PIR Sensor Output In Presence of Motion of a Heat Source In The Field Of View 3
3 Murata Surface Mount PIR Sensor and Fresnel Lens Used in the Design 3
4 PIR Sensor Biasing Method for Low Power Consumption 4
5 The Analog Stages For Filtering and Amplifying the Sensor Signal 5
6 Input Stage “A” Bandpass Filter, Gain and Clamp 6
7 Stage “B”; Bandpass Filter And Gain 7
8 Amplified PIR Signal and The Output Signals of The Window Comparator Circuit 8
9 The Window Comparator Circuit Made of Amplifier "C" And "D" of TLV8544 9
10 Adding Hysteresis To The Inverting Comparator 10
11 Adding Hysteresis To The Noninverting Comparator 11
12 PIR Motion Detector Experiment Board, BOOSTXL-TLV8544PIR 12

1 Introduction

Smart building automation systems employ a large number of various sensing nodes distributed throughout small, medium and large infrastructures. The sensing nodes measure motion, temperature, vibration, and other parameters of interest. Wireless nodes are monitored in a central location. Because of the large number of distributed nodes possible in such a system, battery operated nodes designed with cost-effective, nanopower, electronic components are desirable. Typically, the wireless nodes need to run on a single CR2032 coin battery for eight to ten years. The block diagram of a wireless, battery-powered Passive Infrared (PIR) motion detector is shown in Figure 1. Such detectors are widely used in industrial, commercial and residential building automation applications—See TI reference design, TIDA-01398, for more system information.

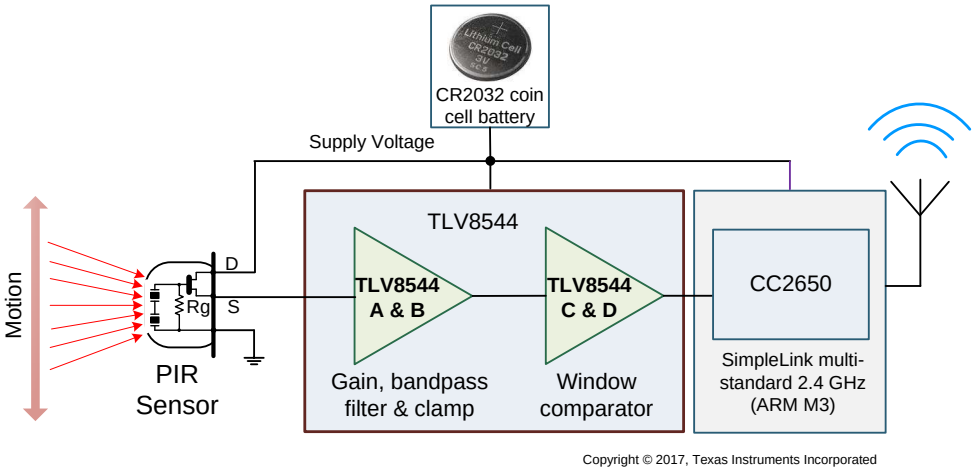

Figure 1. Block Diagram of a Wireless Battery Operated PIR Motion Detector System

In this document, an analog interface circuit for a PIR motion detector, suitable for smart building automation applications, is described. The TLV8544, a new 4-channel nanopower amplifier designed for cost-sensitive systems, is utilized to reduce the power consumption of the sensor node. Configuring two amplifiers of the quad operational amplifier package for amplifying/filtering the signal, and the remaining two amplifiers for implementing a window comparator cost effectively. A booster board, BOOSTXL-TLV8544PIR, for CC2650 Launchpad LAUNCHXL-CC2650 is available from TI website for hands-on experimentation and evaluation of the PIR motion detector circuit.

2 Passive Infrared (PIR) Motion Detector Sensor

The pyroelectric material used in a PIR sensor generates an electric charge when subjected to thermal energy flow through its body [1]. The phenomenon is actually a secondary effect of thermal expansion of the pyroelectrics material, which is also piezoelectric. The absorbed heat by the material causes the front side of the sensing element to expand. The resulting thermally induced stress leads to presence of a piezoelectric charge on the element electrodes. This charge shows up as voltage across the electrodes deposited on the opposite sides of the elements.

Due to the piezoelectric properties of the element, if the sensor is subjected to a slight mechanical stress by any external force, it generates a charge indistinguishable from that caused by the infrared heat waves. For this reason, the PIR sensors are fabricated symmetrically, as shown in Figure 2(b), by placing identical elements inside the sensor's package. The elements are connected to the electronic circuit in a way to produce out-of-phase signals when subjected to the same in-phase inputs. Hence, spurious heat (or external force) signals applied to both electrodes simultaneously (in phase) will be canceled at the input of the circuit, whereas the variable thermal radiation due to motion of a heat source to be detected will be absorbed by only one element at a time, avoiding cancellation. A JFET transistor is used as a voltage buffer and provides a DC offset at the sensor output.

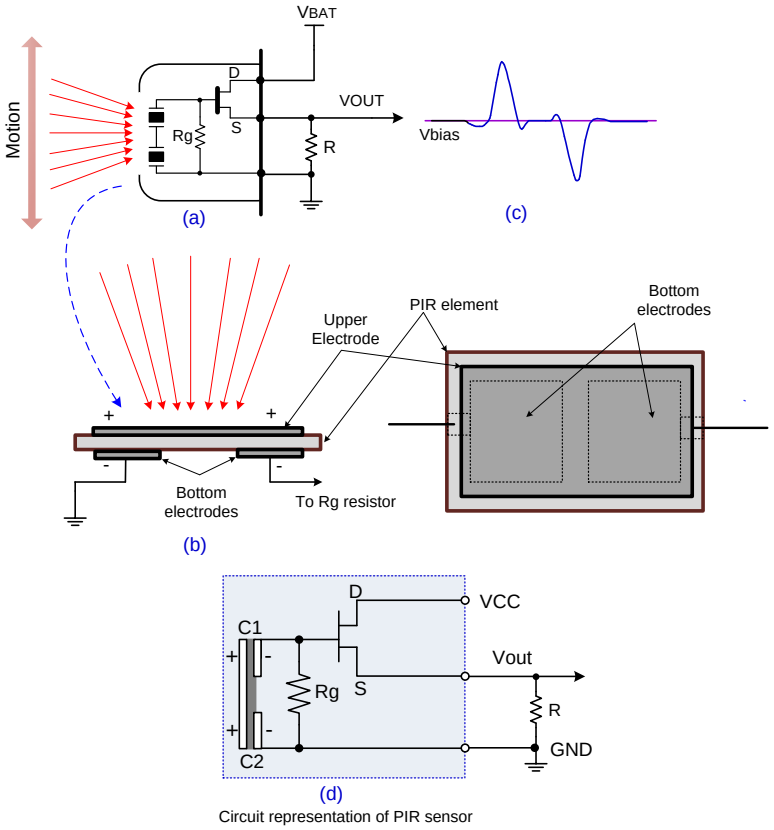

Figure 2. (a) PIR Senor, (b) PIR Transducer, (c) PIR Sensor Output In Presence of Motion of a Heat Source In The Field Of View

The output voltage signal due to a moving object in the sensor's field of view is shown in Figure 2(c). The amplitude of this signal is proportional to the speed and distance of the object relative to the sensor and is in a range of a few hundred microvolts Vp-p up to low millivolts Vp-p. The best sensor response is achieved if it is physically mounded on the board such that the motions are across the elements. Notice that the sensor detects the heat emitted from a source relative to the ambient temperature surrounding the source, therefore, the sensor in the system should be placed away from other sources of time varying high heat such as discharge vents and lamps.

A Murata surface mound (SMD) type PIR sensor [2] and the related lens [3] used in this design is shown in Figure 3. The Fresnel lens is needed in front of the PIR sensor to extend the range of the sensor in a desired field of view. The lens focuses the IR energy onto the small sensor elements in the sensor. Depending on each application, the lens is design for a particular overall viewing angle and detection area coverage.

Murata IRS-B210ST01-R1 Surface mount Pyroelectric, Motion Sensing SMD Module

Murata IML-0669 Fresnel Lens for SMD type PIR

Figure 3. Murata Surface Mount PIR Sensor and Fresnel Lens Used in the Design

The micropower circuit around the PIR sensor typically takes up to 30 seconds to charge all the bypass/feedback capacitors through all the large value resistors. During this time the signal from the last stage is not stable. Therefore, power cycling of the PIR senor and the related analog interface is not practical in motion detection application and the sensor and the interface must be kept "on" continuously.

The bypass capacitor C1 is a critical component because the power supply rejection ratio (PSRR) of the detector is poor (less than 10 dB). Any fluctuation of the supply due to noise will be seen as a signal by the gain stages, resulting in false triggering at the output.

3 Biasing PIR Sensor for Low Power Operation

The PIR sensor supply range is from 2 V to 15 V, in this case about 3V, directly supplied from the battery. As mentioned in the previous section, it must stay on continuously in the system due to its long warm up time from off condition.

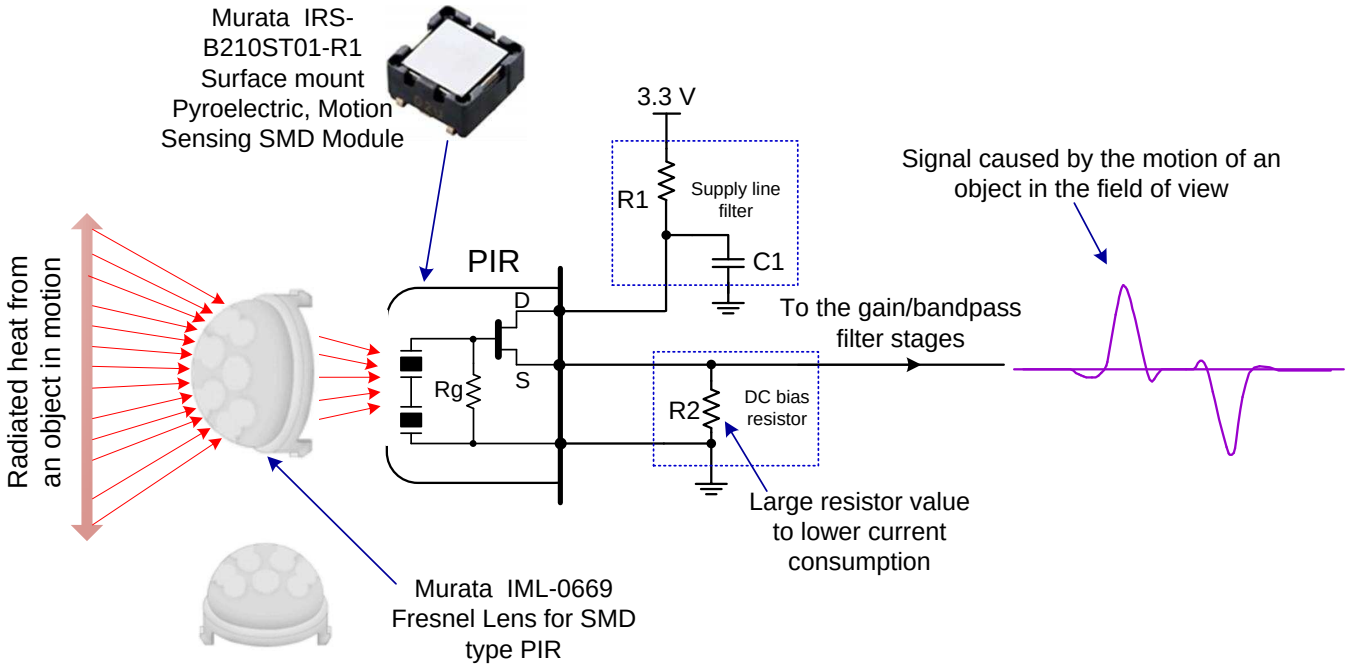

Figure 4. PIR Sensor Biasing Method for Low Power Consumption

As shown in Figure 4, the current through the JFET output transistor of the PIR sensor is controlled by resistor R2, which also, provides the DC bias for the first amplifier stage. Since power cycling of the PIR sensor is not practical, to reduce the current consumption of the sensor substantially, a much larger value (1.3 MΩ) of R2 than the recommended value (47 kΩ) by the sensor manufacturer is used. The penalty is decreased sensitivity and higher output noise at the sensor output, which is a fair tradeoff for increased battery lifetime. To compensate the loss of sensitivity at the sensor output, higher gain value in the filter stages in necessary.

4 Gain Stages and Band Pass Filtering

4.1 Circuit Description

The analog signal path is shown in Figure 5.

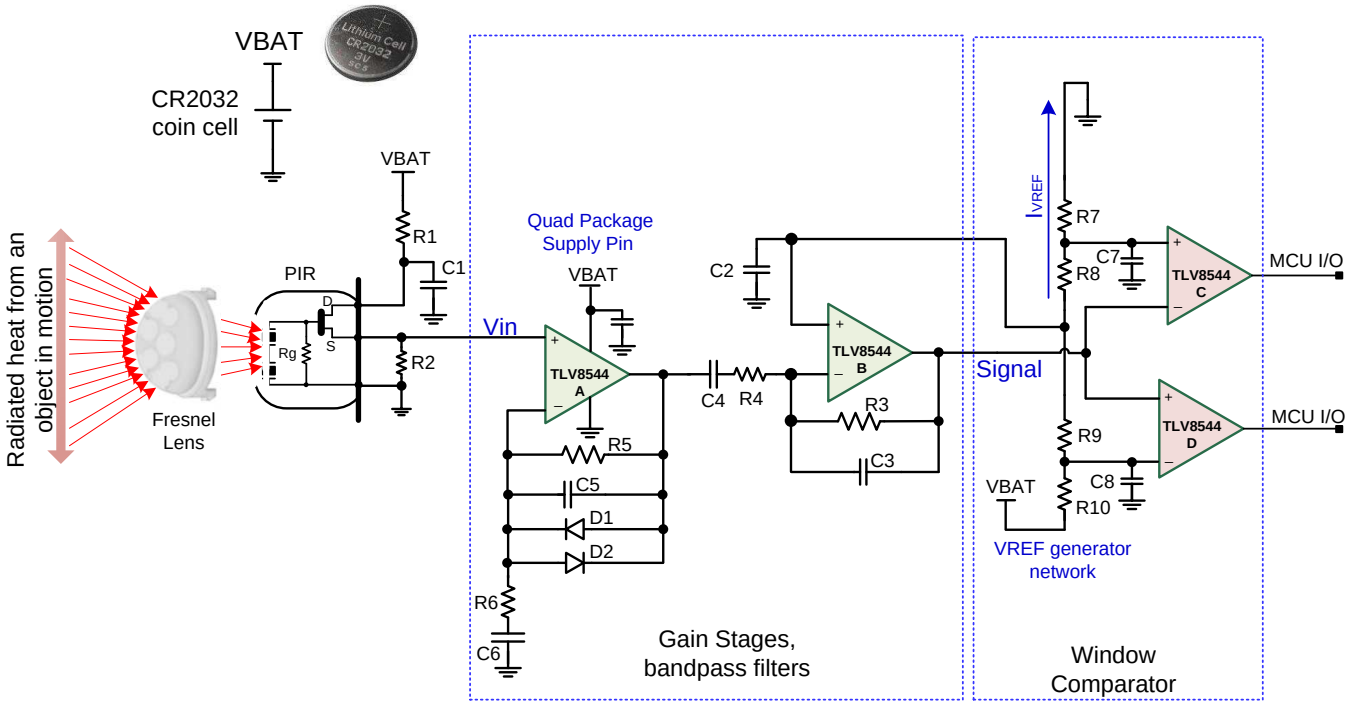

Figure 5. The Analog Stages For Filtering and Amplifying the Sensor Signal

The TLV8544 quad op amp is powered directly by a 3.3 V CR2032 coin battery. The first two amplifier stages of the TLV8544 amplify and filter the signal from the PIR senor. The remaining opamps of the TLV8544 are used for making a window comparator. The comparator signals the detection of a motion event to an ultra-low power wireless microcontroller on the board. Due to the higher gain in the filter stages and higher output noise from the sensor, it is necessary to optimize the placement of the high frequency filter pole and the window comparator thresholds to avoid false detection.

The first two amplifiers (“A” and “B”) in the circuit are used in identical active bandpass filters with corner frequencies of 0.7 and 10.6 Hz. Each filter stage has a gain of about 220 V/V to account for the reduced sensitivity of the sensor due to the low current biasing of the PIR sensor. Considering the 8 kHz unity gain bandwidth (UGBW) product of the TLV8544, the bandwidth of each stage is limited to approximately 36 Hz. The above choice of cutoff frequencies give a relatively wide bandwidth to detect a person running in the field of view, yet narrow enough to limit the peak-to-peak noise at the output of the filters.

Amplifier “A” is a noninverting gain/filter stage, providing the high input impedance needed to prevent loading of the sensor. The DC gain of the stage due to the presence of C6 is unity. Therefore, the sensor output provides the bias voltage needed at the “A” stage to avoid clipping of the lower cycle of the input signal. Diodes D1 and D2 limit the output signal, avoiding over-driving of the second stage, and consequently placing a large charge on coupling capacitor C4, which helps with the recovery time.

4.2 Calculation of the Cutoff Frequencies and Gain Of Stage “A”:

The low cutoff frequency of amplifier "A" is:

$$f_{Clow} = \frac{1}{2\pi \times R_6 \times C_6} \quad (1)$$

Choosing R6 = 6.81 kΩ and C6 = 33 µF, the low cutoff frequency is f_{Clow}= 0.71 Hz. The high cutoff frequency of the filter is:

$$f_{Chigh} = \frac{1}{2\pi \times R_5 \times C_5} \quad (2)$$

For R5 = 1.5 MΩ and C5 = 0.01 µF, the high cutoff frequency is f_{Chigh}= 10.6 Hz. The gain of the stage is:

$$G = 1 + \frac{R5}{R6} \quad (3)$$

Choosing R5 = 1.5 MΩ and R6 = 6.81 kΩ, the gain of the stage “A” is G=221.26 V/V (46.9dB)

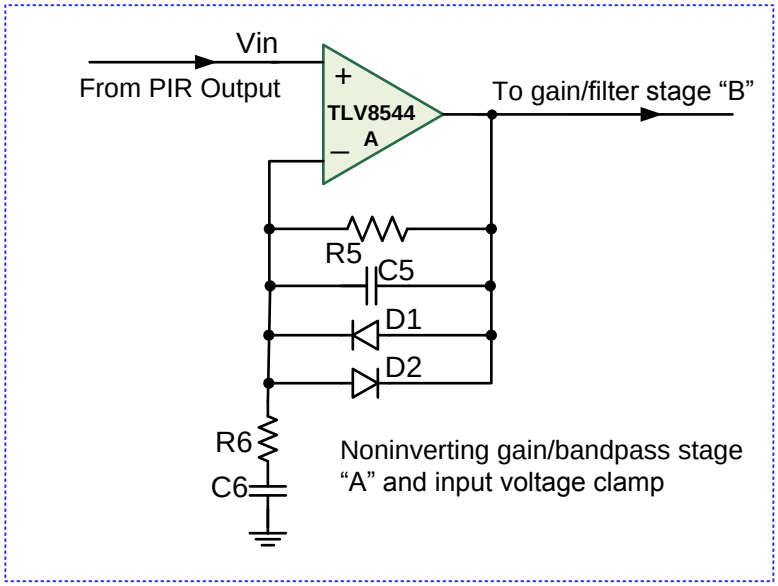

Figure 6. Input Stage “A” Bandpass Filter, Gain and Clamp

4.3 Calculation Of The Cutoff Frequencies And Gain Of Stage “B”

As shown in Figure 7, amplifier “B” is an inverting bandpass filter and gain stage. Capacitor C4 creates an AC coupled path between the “A” and the “B” stages. Thus the signal level must be shifted at the input of the amplifier “B”. This is done by connecting a midpoint voltage of the reference voltage dividers comprising R10, R9, R8 and R7 to the non-inverting input of amplifier “B”, biasing the input signal to the mid-rail (1.65V).

Because the input impedance of the TLV8544 is very high (CMOS input), the positive terminal of the amplifier "B" provides a desired high impedance node for the voltage divider to prevent increase in static current consumption of the reference voltage generator circuit. That is the main reason for using an inverting configuration in stage "B".

A very large feedback resistor R3 is chosen to minimize the dynamic current due to presence of peak-to-peak noise voltage at the output of this stage.

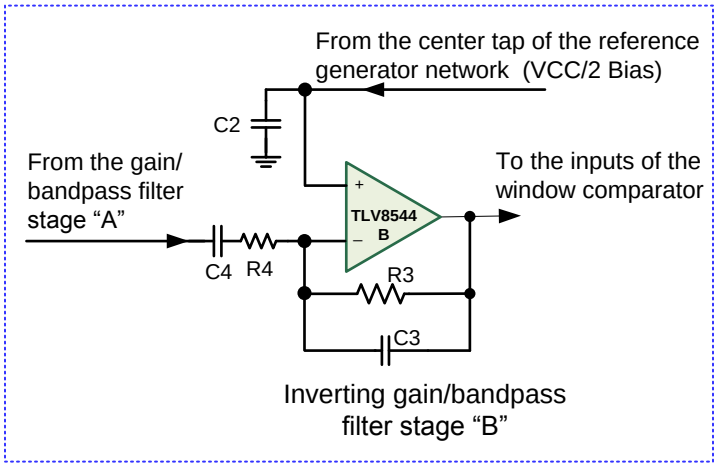

Figure 7. Stage “B”; Bandpass Filter And Gain

The low cutoff frequency of amplifier "B" is:

$$f_{Clow} = \frac{1}{2\pi \times R_4 \times C_4} \quad (4)$$

Choosing R4 = 68.1 kΩ and C4 = 3.3 μF, the low cutoff frequency is, f_{Clow} = 0.71 Hz. The high cutoff frequency of the filter is:

$$f_{Chigh} = \frac{1}{2\pi \times R_3 \times C_3} \quad (5)$$

For R3 = 15 MΩ and C3 = 1000 pF, the high cutoff frequency is, f_{Chigh}= 10.6 Hz. The gain of the stage is:

$$G = -\frac{R3}{R4} \quad (6)$$

For R3 = 15 MΩ and R4 = 68.1 kΩ, the gain is calculated |G|=220.26 V/V (46.9 dB).

5 Calculation Of The Total Gain Of Stages “A” AND “B”

The overall gain of the two stages “A” and “B” is: G_{Total}= G_A*G_B= 221.26*220.26=48810 V/V = 93.77 dB.

6 Window Comparator Stage

The signal from a moving object in front of the PIR sensor, after amplification and filtering, is connected to a window comparator. The comparator converts the analog signal to digital pulses for interrupting an on-board MCU (microcontroller unit), flagging detection of motion. A different approach is to digitize the analog signal continuously by an ADC (analog-to-digital converter) and implement the comparator functionality in the digital domain. This method has the advantage of enabling the post processing of the data to reduce the chance of false detection. However, continuous conversion and processing of data by the MCU increases the power consumption, lowering the battery's life time drastically. Therefore, a window comparator in this case is used to wake up the MCU from power-down state when the PIR signal begins to change due to presence of motion in the field of view.

6.1 Making A Window Comparator With Opamps

Rather than using separate low power comparator integrated circuits to implement the window comparator section of the circuit, the remaining opamps in the TLV8544 package are used to implement the comparator stage. Benefits of this approach include fewer components and thus reduced system cost.

Although an opamp can sometimes be used as a comparator, an amplifier cannot be used as a comparator interchangeably in all applications because of amplifiers’ relatively long recovery time from output saturation and relatively long propagation delay due to internal compensation. Particularly, the nanopower opamps have very slow slew rate, limiting their usage as a comparator in only applications with very low frequency input signal.

The new TLV8544 is particularly suitable for implementing a window comparator in a battery operated PIR motion detector application because of its rail-to-rail operation capability, relatively low offset voltage, low offset voltage drift, very low bias current, and nanopower consumption, all at an optimal cost. The input signal of the comparator stage in the presence of moving heat sources across the sensor is shown in Figure 8. The signal is centered at mid-rail and can swing up or down from the center.

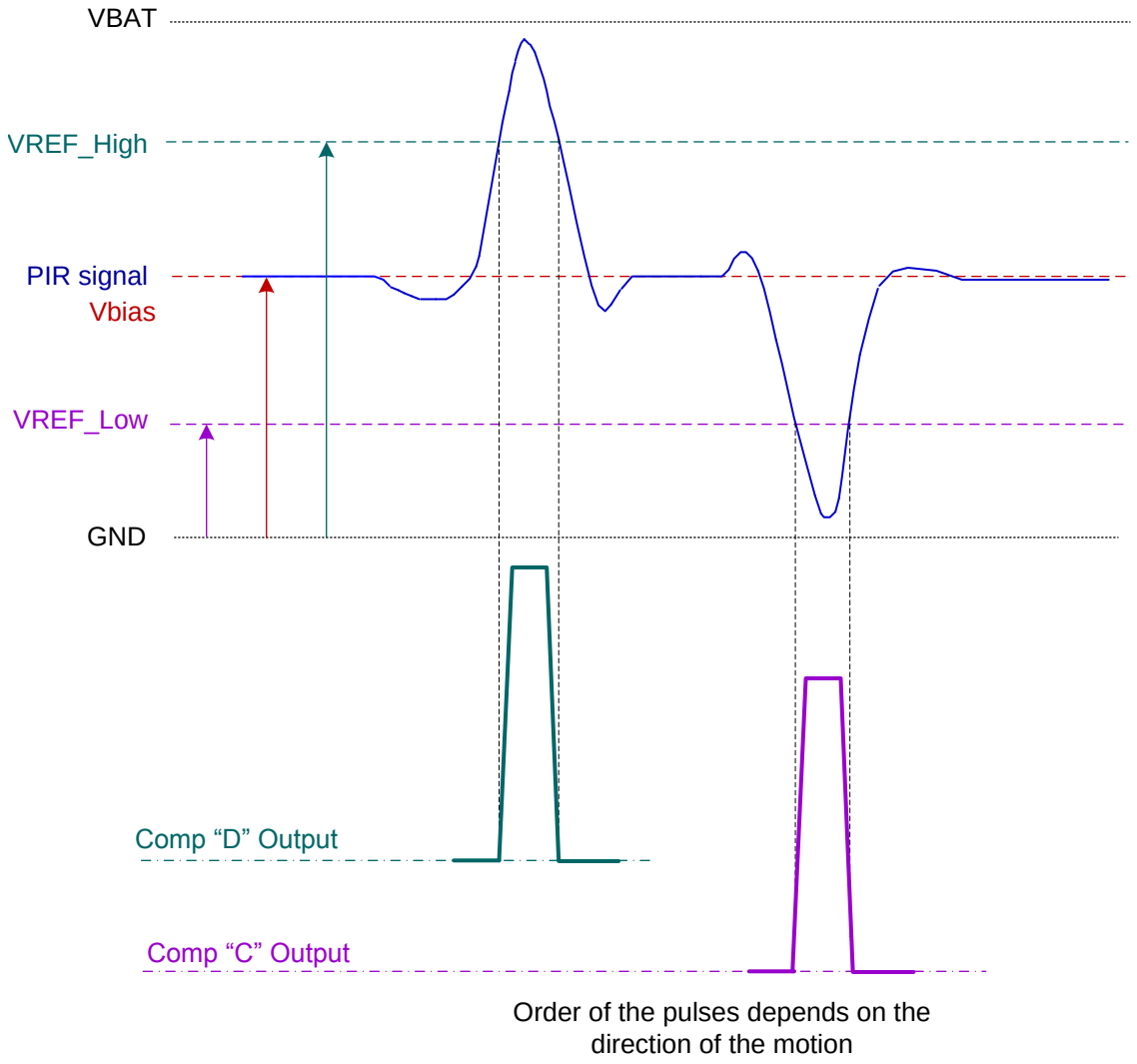

Figure 8. Amplified PIR Signal and The Output Signals of The Window Comparator Circuit

The window comparator is a combination of a non-inverting comparator implemented with amplifier “D” and an inverting comparator implemented with amplifier “C”, as shown in Figure 9.

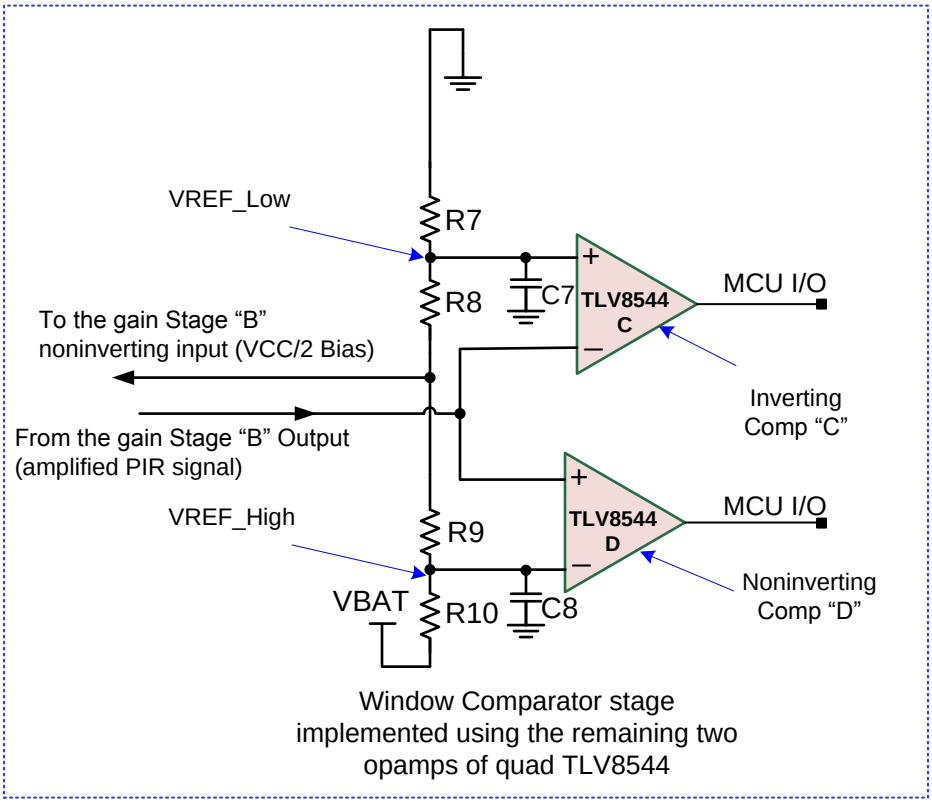

Figure 9. The Window Comparator Circuit Made of Amplifier "C" And "D" of TLV8544

6.2 Reference Voltages

Referring to Figure 9, the divider networks comprising R7, R8, R9 and R10, generate the reference voltages “VREF_High” and “VREF_Low” of the window comparator. The center point of the divider provides the bias voltage of the gain in the stage “B” through the connection to the noninverting input of the amplifier.

Due to the very low bias current of the TLV8544, it is possible to use very large values of resistors in the divider networks to minimize the current to ground through the resistors to a negligible amount. For R7 = R8 = R9 =R10 = 15 MΩ:

$$V_{REF\_High} = \left(\frac{R7 + R8 + R9}{R7 + R8 + R9 + R10}\right) V_{CC} = \frac{4.5 \times 10^6}{6 \times 10^6} \times V_{CC} = 0.75 \times V_{CC} \quad (7)$$

$$V_{REF\_Low} = \left(\frac{R7}{R8 + R9 + R10 + R7}\right) V_{CC} = \frac{1.5 \times 10^6}{6 \times 10^6} \times V_{CC} = 0.25 \times V_{CC} \quad (8)$$

Low leakage ceramic capacitors C7 and C8 maintain constant threshold voltages, preventing potential chatter at the output of the comparators. The comparator outputs stay low in the absence of motion across the sensor. In the presence of motion, comparators ”C” and “D” generate “high” output pulses as shown in Figure 8. The order of the pulses depends on the direction of the motion in front of the sensor.

6.3 Adding Hysteresis to the Window Comparator

The window comparator of the PIR motion detector described in section does not include hysteresis. This is because the opamps are slow and do not react to narrow transitions on the input line rapidly, and therefore, the circuit works well without adding hysteresis. Additionally, hysteresis would cause increased static current dissipation and interference with the divider function due to the changing input impedance, and would require “uneconomical” hysteresis resistor values (100M or higher). In the event that the reader desires to add hysteresis to the window comparator, at the expense of increased current consumption, the following section describes the circuits for adding hysteresis. For a in-depth coverage of this topic please see the LM139-N Datasheet and the application note SNOA654A "AN-74 LM139/LM239/LM339 A Quad of Independently Functioning Comparators"

6.3.1 Adding Hysteresis to the Inverting Comparator

The inverting voltage comparator circuit with external hysteresis resistors R1 and R2 is shown in (a). The corresponding voltage characteristic is shown in Figure 10(b).

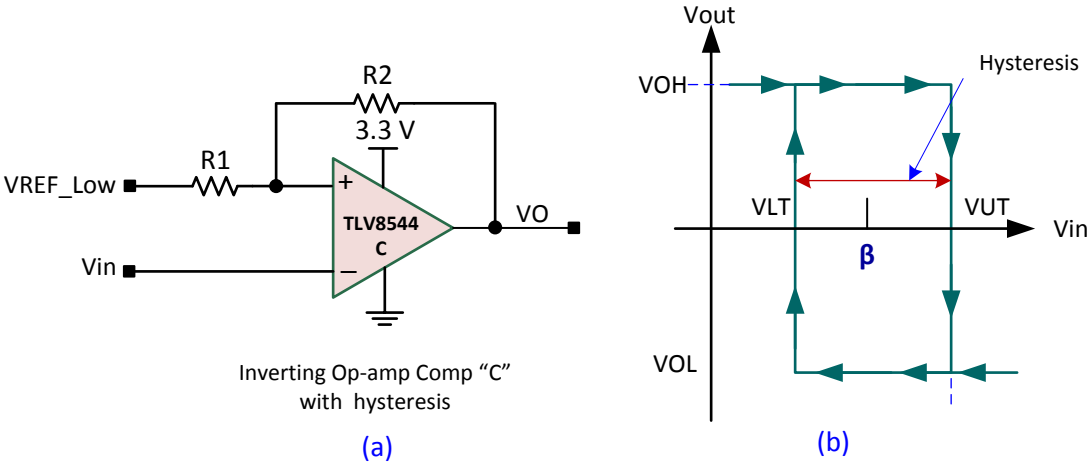

Figure 10. Adding Hysteresis To The Inverting Comparator

The voltage at the noninverting input is [4]:

$$V_{+} = \left(\frac{R2}{R1+R2}\right) \times V_{REF\_Low} + \left(\frac{R1}{R1+R2}\right) \times VO \quad (9)$$

The amount β that the transition voltage is shifted is given by:

$$\beta = \left(\frac{R2}{R1+R2}\right) \times V_{REF\_Low} \quad (10)$$

The upper transition voltage VUT, and the lower transition voltage VLT are given by:

$$V_{UT} = \beta + \left(\frac{R1}{R1+R2}\right) \times VOH \quad (11)$$

$$V_{LT} = \beta + \left(\frac{R1}{R1+R2}\right) \times VOL \quad (12)$$

6.3.2 Adding Hysteresis to the Noninverting Comparator

The noninverting comparator circuit external hysteresis resistors R1 and R2 are shown in Figure 11(a). The corresponding voltage characteristic is shown in Figure 11(b).

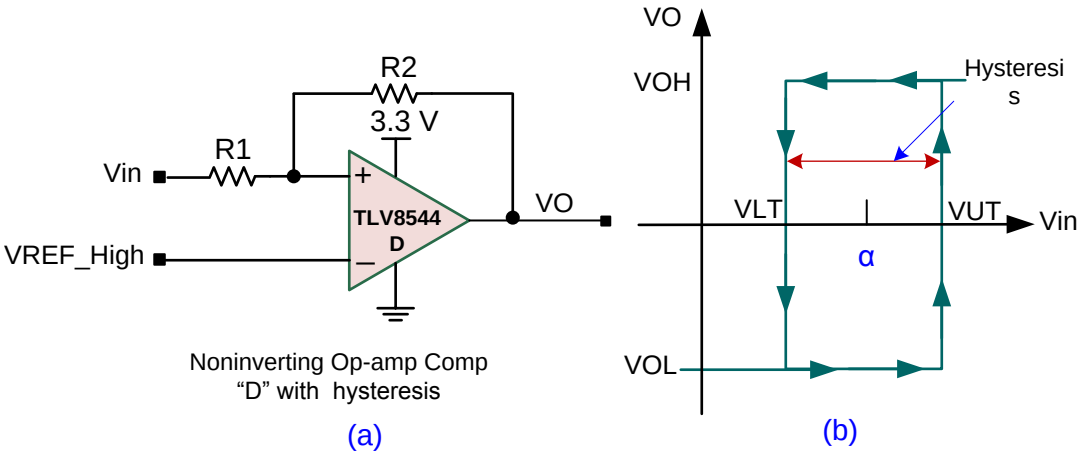

Figure 11. Adding Hysteresis To The Noninverting Comparator

The amount α that the transition voltage is shifted by is given by:

$$\alpha = \left(1 + \frac{R1}{R2}\right) \times V_{REF\_High} \quad (13)$$

The upper transition voltage, VUT, and the lower transition voltage, VLT, are given by:

$$V_{UT} = \alpha - \left(\frac{R1}{R2}\right) \times VOL \quad (14)$$

$$V_{LT} = \alpha - \left(\frac{R1}{R2}\right) \times VOH \quad (15)$$

7 Current Consumption

As previously indicated, ultra-low current consumption is a key requirement for wireless motion detector nodes. The three stages motion detector circuit shown in Figure 5 is powered directly by a single 3.3V CR2032 battery and is optimized for good performance, very low power consumption and optimized cost.

The special biasing of the sensor discussed in this document limits the current consumption of the PIR sensor to 0.5 μA.

The current consumed in the VREF divider circuit is approximately:

$$I_{VREF} = \frac{3.3\ V}{4 * 15^6 \Omega} = 0.055\ \mu A \quad (16)$$

The quiescent current consumption of the TLV8544 is typically 500 nA per channel. The total typical current consumed in the two stages "A" and "B" are approximately:

$$I_{OTLV} = 4 \times 400 \times 10^{-9} = 1.6\ \mu A \quad (17)$$

The total consumption of the analog interface plus the sensor is approximately:

$$I_{Total} = 0.5\mu A + 0.055\ \mu A + 1.6\mu A = 2.16\ \mu A \quad (18)$$

8 Conclusion

Battery operated PIR motion detectors are increasingly used in wireless building automation systems in which nanopower amplifiers for amplification and filtering of the low and noisy signal from PIR sensors are essential.

In this document, a new cost effective quad, nanopower operational amplifier, the TLV8544, was introduced. It was shown how to design the entire analog sensor interface stage, namely amplification, filtering and high- and low- threshold detection, with only a single TLV8544 IC, eliminating the extra cost of additional comparators and components.

The reader is encouraged to obtain and experiment with a PIR motion detector booster board from TI, BOOSTXL-TLV8544PIR shown in Figure 12. The BOOSTXL-TLV8544PIR bundle includes a wireless CC2650 Launchpad board, and the related GUI to interface to a PC, see the board's user's guide SNOU148. The PIR motion detector circuit described in this document is used in the booster board.

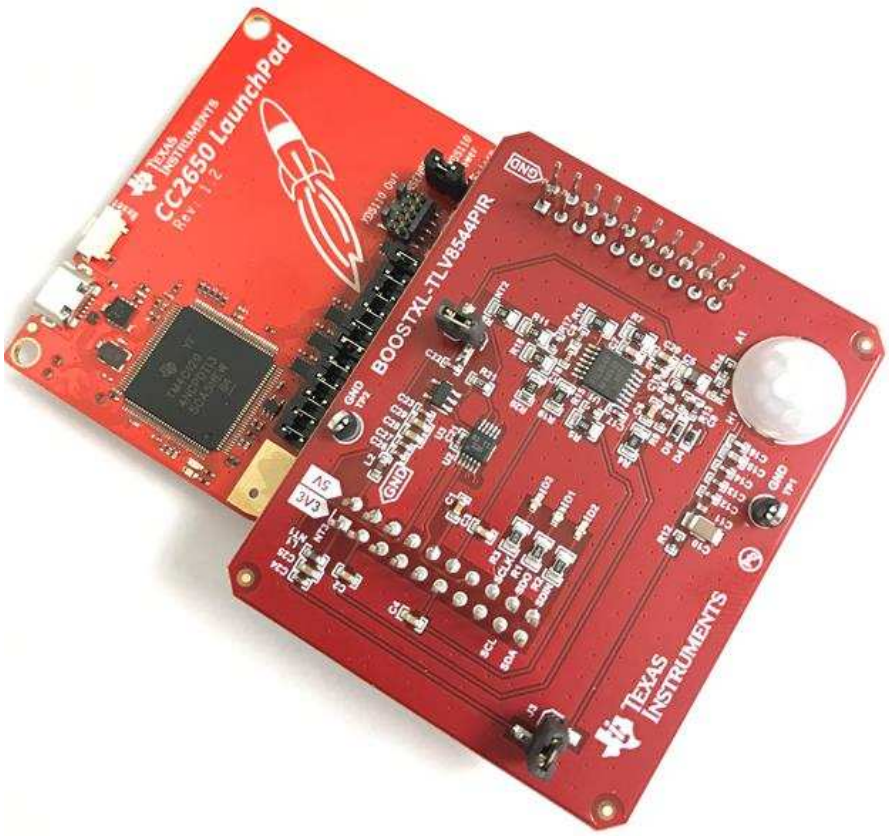

Figure 12. PIR Motion Detector Experiment Board, BOOSTXL-TLV8544PIR

9 Device Family

Table 1. Nanopower Amplifiers Family

Family	Channel Count	IQ/Ch	Vos (max)	Vsupply
TLV854x	1, 2, 4	500 nA	3.1 mV	1.7 to 3.6 V
TLV880x	1, 2	320 nA	4.5 mV	1.7 to 5.5 V
LPV81x	1, 2	425 nA	0.3 mV	1.6 to 5.5 V

10 References

1. Handbook of Modern Sensor; Physics, Design, and applications, third Edition Jacob Fraden, Springer. ISBN 0-387-00750-4
2. Murata IRS-B210ST01-R1 Surface mound Pyroelectric, Motion Sensing SMD Module can be obtained from mouser
3. Murata IML-0669 Fresnel Lens for SMD type PIR
4. Operational Amplifier Circuits; Comparators and positive Feedback. Lecture notes, Chaniotakis and Cory. 6.071 Spring 2006

Revision History

NOTE: Page numbers for previous revisions may differ from page numbers in the current version.

Changes from Original (January 2017) to A Revision	Page
• Changed enhanced the PIR Sensor Biasing Method for Low Power Consumption figure 4	4
• Changed enhanced the Analog Stages For Filtering and Amplifying the Sensor Signal figure 5	4
• Changed enhanced the Input Stage “A” Bandpass Filter, Gain and Clamp figure 6	6
• Changed enhanced the Stage “B”; Bandpass Filter And Gain figure 7	6
• Changed Enhanced The Window Comparator Circuit Made of Amplifier "C" And "D" of TLV8544 figure 9	8
• Changed equation 16	11
• Changed equation 18	11
• Changed Device Family Section	12

IMPORTANT NOTICE FOR TI DESIGN INFORMATION AND RESOURCES

Texas Instruments Incorporated ('TI") technical, application or other design advice, services or information, including, but not limited to, reference designs and materials relating to evaluation modules, (collectively, "TI Resources") are intended to assist designers who are developing applications that incorporate TI products; by downloading, accessing or using any particular TI Resource in any way, you (individually or, if you are acting on behalf of a company, your company) agree to use it solely for this purpose and subject to the terms of this Notice.

TI's provision of TI Resources does not expand or otherwise alter TI's applicable published warranties or warranty disclaimers for TI products, and no additional obligations or liabilities arise from TI providing such TI Resources. TI reserves the right to make corrections, enhancements, improvements and other changes to its TI Resources.

You understand and agree that you remain responsible for using your independent analysis, evaluation and judgment in designing your applications and that you have full and exclusive responsibility to assure the safety of your applications and compliance of your applications (and of all TI products used in or for your applications) with all applicable regulations, laws and other applicable requirements. You represent that, with respect to your applications, you have all the necessary expertise to create and implement safeguards that (1) anticipate dangerous consequences of failures, (2) monitor failures and their consequences, and (3) lessen the likelihood of failures that might cause harm and take appropriate actions. You agree that prior to using or distributing any applications that include TI products, you will thoroughly test such applications and the functionality of such TI products as used in such applications. TI has not conducted any testing other than that specifically described in the published documentation for a particular TI Resource.

You are authorized to use, copy and modify any individual TI Resource only in connection with the development of applications that include the TI product(s) identified in such TI Resource. NO OTHER LICENSE, EXPRESS OR IMPLIED, BY ESTOPPEL OR OTHERWISE TO ANY OTHER TI INTELLECTUAL PROPERTY RIGHT, AND NO LICENSE TO ANY TECHNOLOGY OR INTELLECTUAL PROPERTY RIGHT OF TI OR ANY THIRD PARTY IS GRANTED HEREIN, including but not limited to any patent right, copyright, mask work right, or other intellectual property right relating to any combination, machine, or process in which TI products or services are used. Information regarding or referencing third-party products or services does not constitute a license to use such products or services, or a warranty or endorsement thereof. Use of TI Resources may require a license from a third party under the patents or other intellectual property of the third party, or a license from TI under the patents or other intellectual property of TI.

TI RESOURCES ARE PROVIDED "AS IS" AND WITH ALL FAULTS. TI DISCLAIMS ALL OTHER WARRANTIES OR REPRESENTATIONS, EXPRESS OR IMPLIED, REGARDING TI RESOURCES OR USE THEREOF, INCLUDING BUT NOT LIMITED TO ACCURACY OR COMPLETENESS, TITLE, ANY EPIDEMIC FAILURE WARRANTY AND ANY IMPLIED WARRANTIES OF MERCHANTABILITY, FITNESS FOR A PARTICULAR PURPOSE, AND NON-INFRINGEMENT OF ANY THIRD PARTY INTELLECTUAL PROPERTY RIGHTS.

TI SHALL NOT BE LIABLE FOR AND SHALL NOT DEFEND OR INDEMNIFY YOU AGAINST ANY CLAIM, INCLUDING BUT NOT LIMITED TO ANY INFRINGEMENT CLAIM THAT RELATES TO OR IS BASED ON ANY COMBINATION OF PRODUCTS EVEN IF DESCRIBED IN TI RESOURCES OR OTHERWISE. IN NO EVENT SHALL TI BE LIABLE FOR ANY ACTUAL, DIRECT, SPECIAL, COLLATERAL, INDIRECT, PUNITIVE, INCIDENTAL, CONSEQUENTIAL OR EXEMPLARY DAMAGES IN CONNECTION WITH OR ARISING OUT OF TI RESOURCES OR USE THEREOF, AND REGARDLESS OF WHETHER TI HAS BEEN ADVISED OF THE POSSIBILITY OF SUCH DAMAGES.

You agree to fully indemnify TI and its representatives against any damages, costs, losses, and/or liabilities arising out of your non-compliance with the terms and provisions of this Notice.

This Notice applies to TI Resources. Additional terms apply to the use and purchase of certain types of materials, TI products and services. These include; without limitation, TI's standard terms for semiconductor products http://www.ti.com/sc/docs/stdterms.htm), evaluation modules, and samples (http://www.ti.com/sc/docs/sampterms.htm).

Mailing Address: Texas Instruments, Post Office Box 655303, Dallas, Texas 75265